

SUITABILITY OF EQUIVALENT LINEAR SOIL MODELS FOR ANALYSING THE SEISMIC RESPONSE OF A CONCRETE TUNNEL

Georgios KAMPAS^{1,2}, Jonathan A KNAPPETT², Michael J BROWN², Ioannis ANASTASOPOULOS³, Raul FUENTES⁴, Nikolaos NIKITAS⁴, Andres ALONSO-RODRIGUEZ⁴

ABSTRACT

Current methods of analysis for the seismic response of tunnels rely on linear elastic soil constitutive behaviour. This has obvious benefits in terms of minimising the number of soil parameters required and the complexity compared to more sophisticated soil models. However, it has recently become possible to parameterise sophisticated soil models using only routine data from boreholes or in-situ testing. This paper will therefore review the effectiveness of seismic analyses using an equivalent linear soil constitutive model, by comparison of 2D Finite Element simulations with those using an advanced non-linear elastic model with isotropic hardening plasticity. In the elastic case, the parameters have been estimated using Equivalent-linear Earthquake site Response Analyses software (EERA) and consideration will be given to the amount of sublayering that is required to match the variation of soil properties with depth. The tunnel considered is of horseshoe shape and sprayed concrete construction (New Austrian Tunnelling Method), based on metro tunnels in Santiago, Chile, subjected to the Llolelo ground motion from the 1985 Valparaiso Earthquake. The results will focus the differences in the induced structural forces within the tunnel lining and modification to the ground motion in the near-field of the tunnel, and discuss the implications of this for tunnel design.

Keywords: Finite Element Analysis; Hardening Soil Model; Horseshoe shape tunnel; Seismic Analysis; EERA

1. INTRODUCTION

Underground structures such as tunnels are important transportation systems whose functionality must be maintained following large seismic events. Fortunately, tunnels have suffered damage from earthquakes more infrequently than above-ground structures. The developed inertial forces are not a dominating parameter controlling their dynamic response compared to the applied kinematic loading resulting from the complex soil-structure interaction behaviour (Dowding and Rozen 1978; Wang 1993; Kawashima 2000; Anastasopoulos and Gazetas 2010; Tsinidis et al. 2016). However, some notable cases of significant damage or tunnel collapse signify that under specific circumstances tunnels can experience severe damage due to strong earthquake loading. These include the Daikai subway station in Kobe during the 1995 Hyogoken-Nambu earthquake, several ‘horseshoe-shaped’ tunnels in Taiwan during the 1999 Chi-Chi earthquake and the Bolu tunnels in Turkey during the 1999 Kocaeli earthquake (Iida et al. 1996; Nakamura et al. 1996; Ueng et al. 2001; O’Rourke et al. 2001; Anastasopoulos and Gazetas 2010; Hashash 2011; Kontoe et al. 2011).

However, the seismic analyses of tunnels involve many parameters and can become quite complex. The level of complexity together with the number of available input soil properties has made simpler soil constitutive models more popular to practitioner engineers. Kontoe et al. (2011) has conducted a very thorough investigation comparing different models ranging from simple constitutive models to more sophisticated regarding clay soil and circular tunnels.

Hence, this paper investigates the efficiency of seismic analyses using equivalent linear models compared to more sophisticated soil models with respect to HST95 sands (Al-Defae et al., 2013). The

¹ University of Greenwich, Chatham, UK, G.Kampas@gre.ac.uk

² Former University of Dundee, Dundee, UK

³ ETH, Zurich, Switzerland

⁴ University of Leeds, Leeds, UK

tunnel considered will be horseshoe-shaped, inspired by real sprayed-concrete (NATM) Metro tunnels in coarse-grained soils in Santiago, Chile which have recently been constructed. A series of numerical analyses will be undertaken using the Finite Element Method using a constitutive soil model that accounts for both nonlinear pre-yielding behaviour and post-yielding isotropic hardening, and which has been previously validated against centrifuge data for a range of seismic soil-structure interaction problems on non-liquefiable sand (including slopes – Al-Defae et al., 2013; above-ground structures – Knappett et al., 2015 and tunnels – Lanzano et al., 2015). More specifically, the 3 constitutive models compared in this study are: a) the Linear Elastic model (LE model) with Rayleigh damping to compensate for its inability to exhibit hysteretic behavior, b) the Mohr-Coulomb model (MC model) which uses the same properties as the LE model but can yield following the Mohr-Coulomb criterion and c) the aforementioned hardening soil model with small-strain stiffness (“HS small” model) that accounts for the pre-yielding nonlinear behavior of the soil together with the post-yielding isotropic hardening. The paper focuses on presenting the results regarding the accelerations and amplification ratios at the ground surface and the lining forces.

2. MODEL DESCRIPTION

2.1 Finite element analysis

The chosen software for the seismic analyses of the tunnel is PLAXIS 2D. The numerical model developed for this purpose is shown in Fig. 1. The soil layer’s depth is approximately 7 times the height of the tunnel $z = 56.6m \approx 7H_{tunnel}$ while the width of the total model is approximately 40 times the width of the tunnel, $W_{model} = 430m \approx 40 \times W_{tunnel}$ for avoiding undesired boundary effects (Amorosi and Boldini 2009; Amorosi et al. 2010). The cover depth of the tunnel is $C \approx 18m$. The abovementioned soil profile is based on a real Metro tunnel section in Chile.

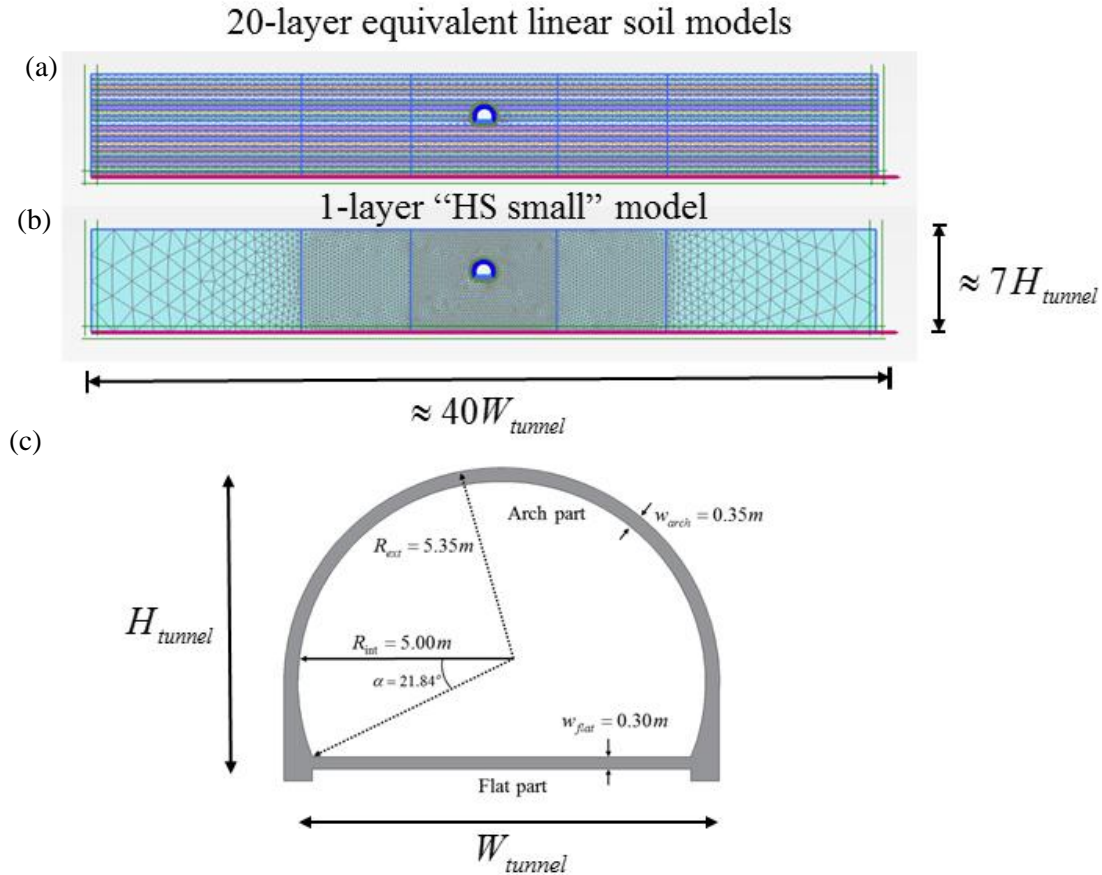


Figure 1. The numerical model used in this study: (a) the mesh of an equivalent linear 20-layer soil model, (b) the mesh of a single-layer nonlinear soil model and (c) the tunnel section. The mesh has three main zones of different local refinement as shown in Fig. 1. The total number of

triangular 15-node plane-strain finite elements is 7,910 which resulted after multiple iterations until the response reaches a convergence.

Furthermore, the boundaries used in this model are viscous boundaries proposed by Lysmer and Kuhlmeyer (1969) with relaxation coefficients $C_1 = 1$ and $C_2 = 0.25$ along the horizontal and the vertical direction, respectively. The two different values of viscosity are proposed by PLAXIS 2D for dynamic analyses. Viscous boundaries are very commonly used for dynamic and seismic analyses since they tend to absorb the generated seismic waves rather than reflecting them back and thus creating spurious amplification effects. The algorithm for solving the equation of motion used by PLAXIS is Newmark numerical scheme (Newmark 1959; Chopra 2001, amongst others) with coefficients, $\alpha_N = 0.25$, $\beta_N = 0.50$ using the average acceleration method.

Regarding damping (Zerwer et al. 2002; Kwok et al. 2007; Kontoe et al. 2011, amongst others) this study considers two major energy dissipative mechanisms: (a) hysteretic damping through the nonlinear soil behaviour as described in the next section and (b) frequency-dependent Rayleigh damping given by

$$[C] = c_m[M] + c_k[K] \quad (1)$$

where, $[C]$ is the damping coefficient matrix, $[M]$ and $[K]$ are the mass and stiffness matrices of the model respectively. The parameters c_m and c_k are the Rayleigh coefficients set to $c_m = 0.0005$ and $c_k = 0.005$ as proposed by Al-Defae et al. (2013) for sands based on thorough centrifuge testing.

2.2 Soil profiles

The behavior of the soil is best represented by a nonlinear soil model with isotropic hardening (Schanz et al. 1999) called “hardening soil model with small-strain stiffness” (Benz 2006) in PLAXIS (HS small model). The pre-yielding part of the model is following a nonlinear relation between the shear modulus, G , and the shear strain, γ_s , proposed by Hardin and Drnevich (1972) and later modified by Santos and Correia (2001) as

$$\frac{G}{G_0} = \frac{1}{1 + 0.385 \left| \frac{\gamma_s}{\gamma_{s,0.7}} \right|} \quad (2)$$

where G_0 is the shear modulus corresponding to small strains and $\gamma_{s,0.7}$ is the shear strain that corresponds to $G/G_0 = 0.722$. Plasticity is introduced as a cap-type yield surface combined with a Mohr-Coulomb failure criterion (Smith and Griffiths 1982).

For representing coarse-grained soils, this study considers dry sands from the HST95 dataset (Lauder, 2011; Bransby et al., 2011; Al-Defae et al., 2013) with relative density $D_r = 60\%$ for conducting the analyses. Except the nonlinear relation of the shear modulus, G , with the shear strain, γ_s , the soil model accounts also for the variation of G_0 with depth, z as shown below and in Fig.2,

$$\frac{G_0}{G_0^{ref}} = \left(\frac{c' \cos \varphi' - \sigma_3' \sin \varphi'}{c' \cos \varphi' + p_{ref} \sin \varphi'} \right)^m \quad (3)$$

where G_0^{ref} is the shear modulus corresponding to small strains at the reference pressure point of $p_{ref} = 100kPa$, c' is the apparent cohesion value, φ' is the friction angle, σ_3' is the effective confining stress and m is an empirical parameter controlling the shape of the relation.

The “HS small” model requires 11 input parameters as shown in Table 1: unit weights under saturated and dry conditions, γ_{sat} , γ_d ; 5 stiffness parameters (which are stress dependent): the secant stiffness in drained triaxial test, E_{50} , the tangent stiffness for primary oedometer loading, E_{oed} , the unloading-reloading stiffness from drained triaxial test, E_{ur} , the small-strain stiffness, G_0^{ref} , and the shear strain

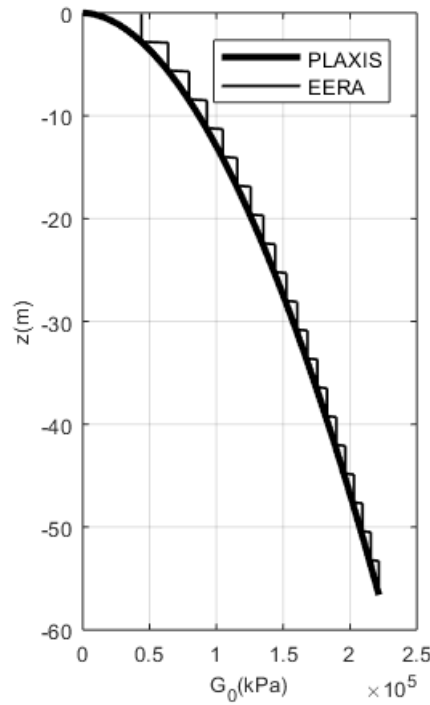


Figure 2. Initial distribution of the shear modulus, G , with depth, z for single-layer model in PLAXIS and equivalent linear 20-layer model in EERA.

that corresponds to $G/G_0 = 0.722$, $\gamma_{s,0.7}$; 3 strength parameters: c' , φ' , ψ , apparent cohesion, friction and dilatancy angles respectively; and 1 empirical parameter, m , controlling the variation of shear stiffness with confining stress as shown in eq. (3). The values of those parameters according to HST95 are shown in Table 1. Furthermore, this paper assumes that the water table is below the tunnel's inverse and thus there is not a possibility for liquefaction.

2.2.1 Equivalent-linear Earthquake site Response Analysis (EERA)

The other two soil profile considerations were based on estimating the equivalent linear soil models. Thus, given a specific soil profile (shown in Fig. 1), a material constitutive law and an excitation, the Equivalent-linear Earthquake site Response Analysis (EERA – Bardet et al. 2000) software is applying an iterative algorithm to converge to the equivalent linear response of the soil profile and the corresponding linear parameters associated with the specific constitutive law and excitation.

Figure 2 shows a comparison of the two shear moduli distributions for PLAXIS 2D and for the 20-layer soil profile developed in EERA. The selection of 20 layers was arbitrary as an engineer can use any number of layers that could fit adequately to the shear modulus distribution with depth.

More specifically, the algorithm for developing the Linear Elastic (LE) and Mohr-Coulomb (MC) equivalent models is described below:

- 1) Definition of the soil profile (and the number of layers), the material constitutive law (eq. 2) and the three excitations (described in the next section) in EERA.
- 2) Run iterative analysis that finds the equivalent linear response of the profile in reference.
- 3) Get as an output the equivalent shear modulus and damping ratio for each layer
- 4) Assign the equivalent shear modulus, G_i , and damping ratio, ξ_i , values to each layer in PLAXIS 2D using the Linear Elastic (LE) material. The ξ_i are assigned on the two first natural frequencies of the soil profile based on the Fourier spectra of its response.
- 5) Assign the equivalent shear modulus, G_i , and damping ratio, ξ_i , values to each layer in PLAXIS 2D using the Mohr-Coulomb (MC) material.
- 6) Run the seismic analyses of the LE and MC models for the three different excitations defined in the section below.

Table 1. Parameters' values for HST95 sand with relative density $D_r = 60\%$.

HST95 Parameters	$D_r = 60\%$
unit weight, $\gamma_d (kN/m^3)$	16.30
saturated unit weight, $\gamma_{sat} (kN/m^3)$	19.88
secant stiffness in drained triaxial test $E_{50} (kPa)$	44,025
tangent stiffness for primary oedometer loading $E_{oed} (kPa)$	35,220
unloading-reloading stiffness, $E_{ur} (kPa)$	105,600
small-strain stiffness, $G_0^{ref} (kPa)$	118,800
shear strain, $\gamma_{s,0.7}$	1.7×10^{-4}
friction angle, $\varphi' (^{\circ})$	41.00
dilatancy angle, $\psi (^{\circ})$	11.20
Apparent cohesion, $c' (kPa)$	0 or 50
m	0.54

2.2.2 Linear Elastic soil model (LE model)

The LE soil model is the crudest approach to modelling a soil layer. It is based on Hooke's law of isotropic elasticity and the input parameters are the shear modulus, G , Poisson's ratio, ν , and damping ratio, ξ , for each individual layer (PLAXIS Materials' Manual 2016).

2.2.3 Mohr-Coulomb soil model (MC model)

On the other hand, the Mohr-Coulomb model (MC model) is the most well-used soil model. It is an elastic perfectly-plastic model that uses a Mohr-Coulomb yielding criterion (Smith and Griffiths 1982; Vermeer and Borst 1984). Due to its constant stiffness, computations tend to be faster than the HS small model. The MC model requires 5 parameters; 2 regarding the soil stiffness: shear modulus, G and Poisson's ratio, ν , and 3 associated with soil strength: c' , φ' , ψ , apparent cohesion, friction and dilatancy angles respectively, as in the case of the "HS small" model.

2.3 Tunnel section

The tunnel is represented by a reinforced concrete horseshoe type of section as shown in Fig. 1. This is a typical section for Metro tunnels in Chile where the first part of the section is circular with constant radius, $R = 5.35m$, (arch part) intersecting at the bottom with a classic beam (flat part). This connection is called the "elephant's foot" by tunnel engineers. In this study, tunnel structural elements are considered linear elastic reinforced concrete plate elements with $EI_{arch} = 91,980kNm^2$ and $EI_{flat} = 57,920kNm^2$ for the arch and the flat part, respectively.

2.4 Ground motions

This paper investigates the seismic behavior of the soil profile of Fig. 1 when subjected to the Takarazuka/000 record from the 1995 Kobe earthquake ($M_w = 6.9$) scaled at $a_g = 0.20g$, $0.45g$ and $0.69g$ (TK-0.20g, TK-0.45g, TK-0.69g, respectively) as shown in Fig. 3. The record was downloaded from the PEER NGA Strong Motion Database (<http://ngawest2.berkeley.edu/>). Fig. 3b illustrates the response spectra of the scaled TK records accordingly for damping ratio, $\xi = 5\%$.

3. SEISMIC ANALYSES

The results from the seismic analyses conducted are presented into two different sections: Accelerations and Lining forces.

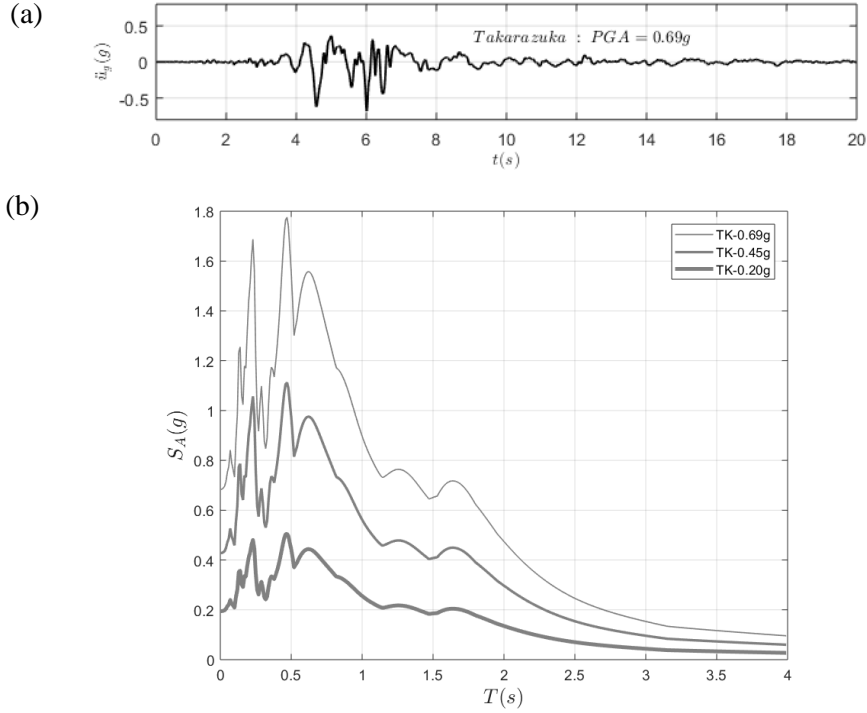


Figure 3. (a)Takarazuka/000 record from the 1995 Kobe earthquake; (b)Response spectra corresponding to the TK-0.69g, TK-0.45g and TK-0.20g ground motions for $\xi = 5\%$.

3.1 Accelerations

Fig. 4 illustrates the settlement and the acceleration response at the ground surface above the tunnel centreline, the acceleration below the tunnel and the corresponding excitation for the three different soil models when subjected to the TK-0.69g excitation.

One of the main advantages of the "HS small" model is that it can provide information about the post-earthquake settlement compared to the other two models that are not capable of capturing accurately post-earthquake settlements. The settlements observed in Fig. 3a are reaching almost 100mm; this is a very large value but comes as a result of a quite significant earthquake. Fig. 3b shows that all models have the same order of magnitude accelerations without any big amplification at the ground surface. However, there is a small discrepancy between the MC and the LE soil models as the MC yields following the Mohr-Coulomb criterion when subjected to such severe record. On the other hand, Fig. 3c shows that closer to the vicinity of the tunnel there is a bigger difference in the values of the accelerations between the "HS small" model and the equivalent MC and LE models; a result that reflects on differences in the lining forces.

Fig. 5a presents the free-field amplification values, S_{FF} , representing the ratio between the maximum acceleration response on the ground surface over PGA. Interestingly, a decrease of S_{FF} is observed with PGA in agreement with Knappett et al. (2015) for all soil models. Furthermore, the discrepancy between the amplification values for the different soil models tends to remain constant for all PGA values. However, the equivalent linear soil models (MC and LE) overestimate the response for small PGA values, while, underestimate the response at the ground surface for medium to large values of PGA. Fig. 5b shows the near-field amplification values, S_{NF} , following the same trend with the S_{FF} , although, $S_{NF} > S_{FF}$ for small PGA highlighting the effect of the tunnel existence on the ground surface. Another observation that can be extracted from Fig. 5b is that the discrepancies between the "HS small" model with the MC and LE models are decreasing with increasing PGA. This is a significant result showing the effect of the pre-yielding nonlinearity on small to medium PGA values (more frequent earthquakes).

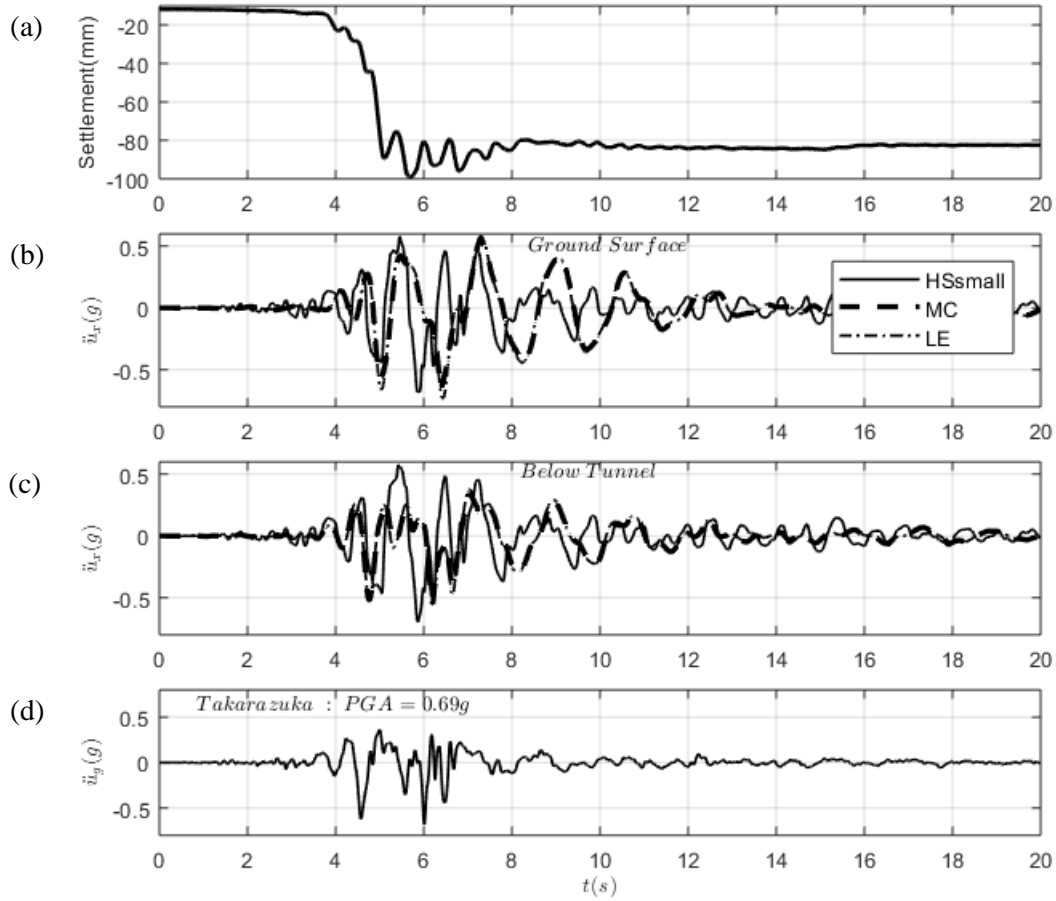


Figure 4. (a) Settlements and (b) accelerations at the ground surface, (c) accelerations below the tunnel for the HS small, MC ad LE soil models respectively when subjected to the (d) TK-0.69g ground motion.

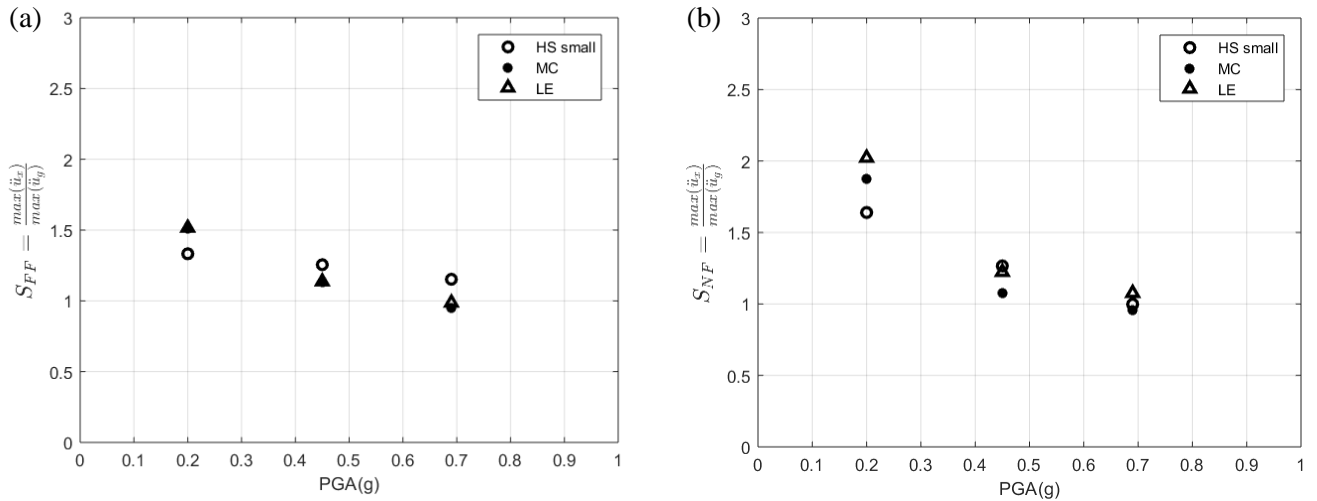


Figure 5. (a) Free-field, S_{FF} , and (b) near-field, S_{NF} , amplification values as a function of the Peak Ground Acceleration (PGA).

3.2 Lining Forces

Fig. 6 presents the maximum internal forces developed on the arch and the flat part of the horseshoe shape tunnel of Fig. 1c. The MC and LE models exhibit a more symmetrical distribution of maximum axial forces on the arch and the flat part. Interestingly, the “HS small” model’s results regarding the

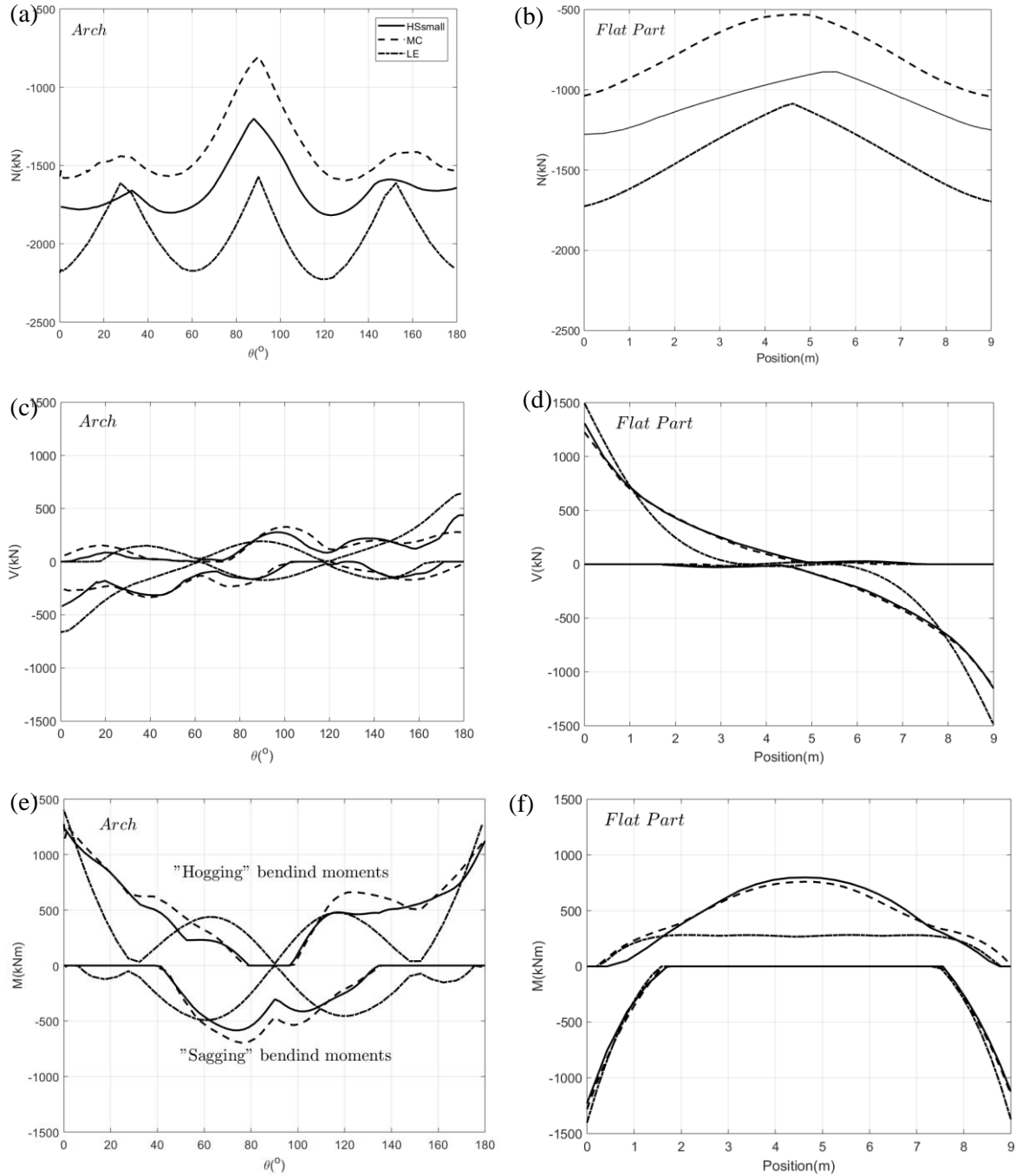


Figure 6. Axial (circumferential) force, N , (a) of the arch part and (b) of the flat part of the tunnel section; Shear force, V , (c) of the arch part and (d) of the flat part of the tunnel section; Bending moment, M , (e) of the arch part and (f) of the flat part of the tunnel section varying with angle, θ , for the arch part and with position for the flat part in the case of the TK-0.69g excitation. Note: The bending moment plots (e-f) convention follows the deformed shape of the lining, thus the negative moments signify tension on the bottom side of the structural element.

circumferential (axial) forces are placed between the MC and the LE models. The LE model exhibits the most conservative results compared to the MC and HS small models regarding both the axial and shear forces. An interesting observation can be deduced from Fig. 6f,e as the bending moments do not follow the abovementioned trends; the MC and “HS small” models exhibit more conservative results especially having to do with the flat part of the section. The reason behind this result is related to the dilation of the soil around the tunnel and the application of additional dynamic kinematic loading to the tunnel.

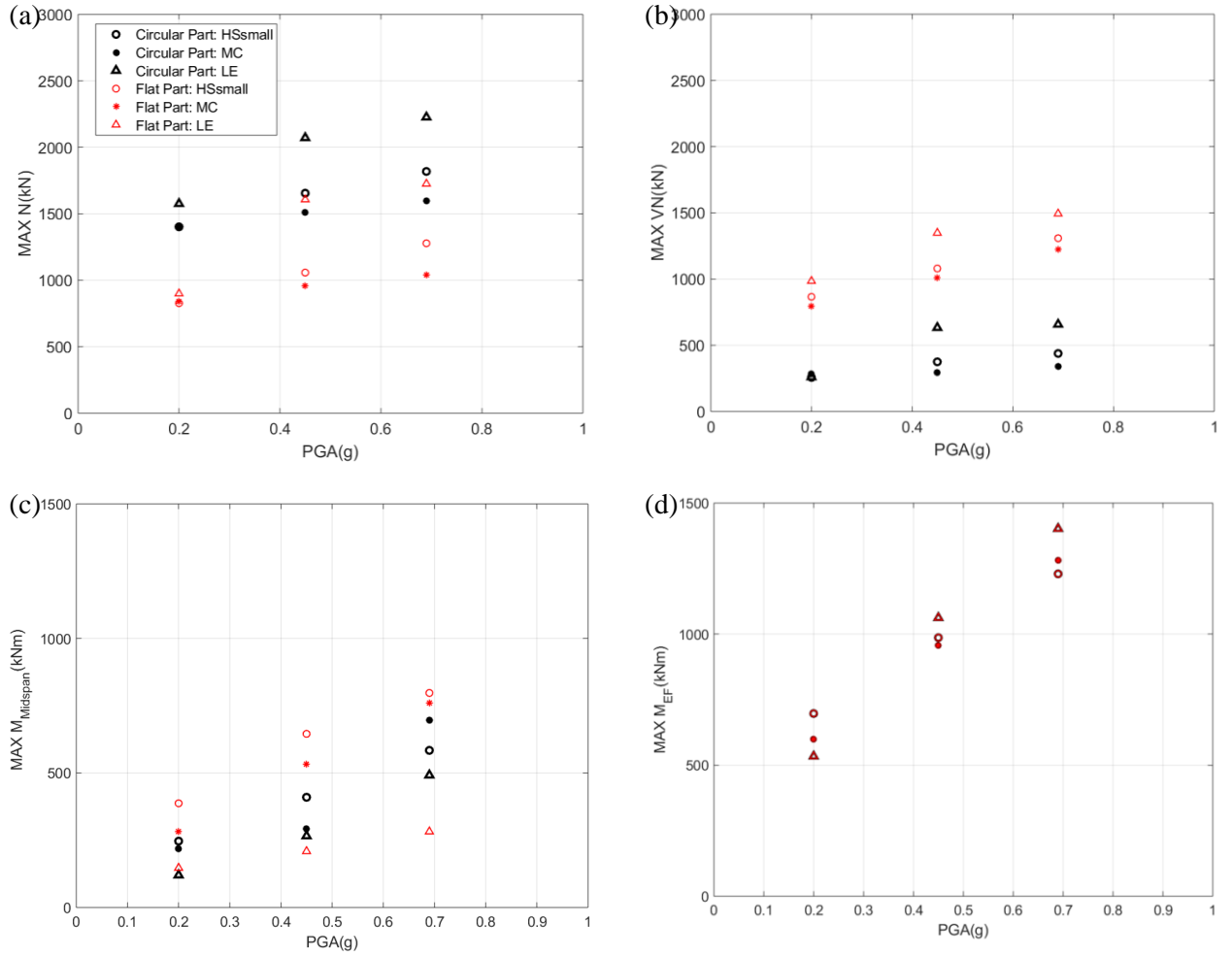


Figure 7. (a) Maximum circumferential force, N ; (b) shear force, V ; (c) "midspan" bending moment, $M_{midspan}$; and (d) "elephant's foot" bending moment, M_{EF} , for both the arch and the flat parts of the tunnel section with respect to PGA.

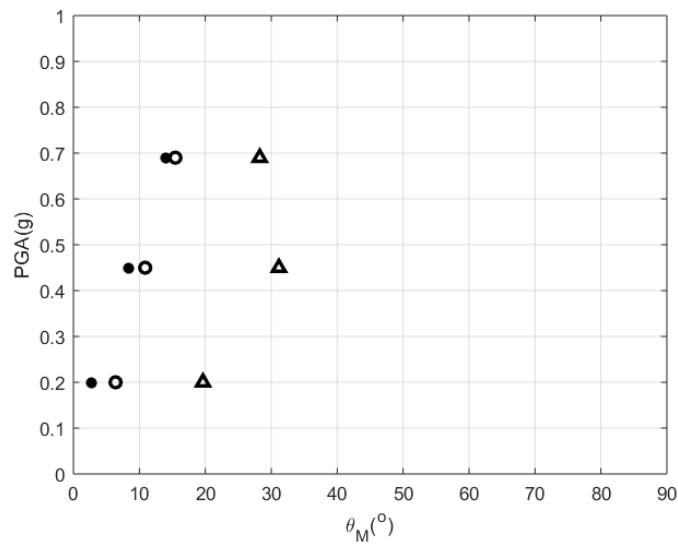


Figure 8. Location of the maximum "midspan" bending moments, $|M_{midspan,max}|$, measured as an angle from the tunnel crown, $|\theta_M|$, against PGA for the HSsmall, MC, and LE cases.

Fig. 7 presents the maximum lining forces developed in the tunnel with respect to PGA. Obviously, the values of all lining forces are proportional to PGA. More specifically, Fig. 7a illustrates that the maximum circumferential forces developed in the arch part are bigger than the flat part, while, Fig. 7b shows that the shear forces on the flat part are always higher than the arch part; a result, that can be expected as arches and typical beams tend to perform differently as structural forms. Additionally, the maximum axial and shear force of the LE model is the highest (most conservative) and of the MC model is the lowest (most non-conservative).

On the other hand, Fig. 7c presents that the bending moments at the midspan of both the arch and flat part in the case of the “HS small” model provides the most conservative result most times. The bending moment at the midspan of the flat part is related to the nonlinear and yielding behavior of the soil that applies an upward pressure on the flat part of the tunnel and thus the LE model is unable to capture that. Fig. 7d confirms that the bending moments at the “elephant’s foot” coincide for both the arch and the flat part.

Finally, Fig. 8 presents the location of the maximum bending moments near the midspan, $M_{midspan}$, of the arch part; information that is particularly useful for the engineers involved with the detailing of the reinforcement along the arch. The location is presented as an angle, θ_M , from the tunnel’s crown (where $\theta_M = 0$). “HS small” and MC models exhibit very similar locations for their maxima, while, LE model’s maxima exhibit an offset from the tunnel’s centreline. Another interesting observation is that as the PGA increases, the maximum “midspan” bending moments drift apart from the tunnel’s crown.

5. CONCLUSIONS

This paper investigates the suitability of equivalent linear soil models that are able (MC model) and unable (LE model) to yield for conducting seismic analyses for a concrete-sprayed tunnel surrounded by sand. The benchmark model was a single-layer soil profile model using the “hardening soil model with small-strain stiffness” or “HS small” model for capturing the pre-yielding nonlinear response of the soil along with an isotropic hardening behaviour after yielding, while, the two equivalent linear soil models were developed with the use of EERA.

One major difference with the use of the different soil models is that the equivalent linear models are not able to estimate reliably the post-earthquake settlements that can be of great importance for the seismic resilience of the above-ground infrastructure.

Regarding accelerations, the near-field amplification values were higher than the free-field amplification values for small to medium values of PGA illustrating the effect of the tunnel at the ground surface, although their values drop with increasing PGA. Nevertheless, the discrepancy of the amplification values for the different soil models is higher for small to medium values of PGA (most frequent earthquakes) with the LE model exhibiting the largest value (most conservative); the reason behind the major difference between the LE and the “HS small” model is the effect of the pre-yielding nonlinearity of the soil captured only by the “HS small” model.

An interesting observation regarding lining forces is that the maximum circumferential forces developed on the arch part of the tunnel are higher than the ones on the flat part, while the exact opposite result is observed for shear forces. This result highlights the difference in the performance of an arch and a typical beam as different structural forms. Additionally, the LE model provided the most conservative results because it did not account for soil yielding but the MC model -which is widely used in practice- provided the most non-conservative results in most cases. Furthermore, the location of the maximum midspan bending moments for the arch part are different in the case of the LE model with respect to the MC and “HS small” models.

Finally, this paper concludes that the LE model is not appropriate for the modelling of the soil as the results have big differences with the more sophisticated soil models, while, it proves as the most conservative model in total. The MC model is not appropriate for modelling the soil when focusing on the seismic resilience of the above ground structures due to the existence of the tunnel. However, regarding the design of the tunnel itself, if the soil profile is discretized appropriately (in this case with 20 layers) and with the addition of a safety factor, especially when designing for high return period earthquakes (high PGA), the model could prove to give comparable results to the more sophisticated “HS small” model.

6. ACKNOWLEDGMENTS

This project was funded by the Newton Fund: EPSRC, UK & CONICYT Chile: Shaking tunnel vision. Joint project led by University of Leeds EP/N03435X/1.

7. REFERENCES

- Al-Defae, AH, Caucis, K. & Knappett, JA (2013). Aftershocks and the whole-life seismic performance of granular slopes. *Geotechnique* 63(14): 1230–1244.
- Amorosi A, Boldini D (2009). Numerical modelling of the transverse dynamic behaviour of circular tunnels in clayey soils. *Soil Dyn Earthq Eng*, 29(6):1059–72.
- Amorosi, A., Boldini, D., and Gaetano, E., (2010). Parametric study on seismic ground response by finite element modelling. *Computers and Geotechnics*, 37 :515-528.
- Anastasopoulos, I, and Gazetas, G., (2010). Analysis of cut-and-cover tunnels against large tectonic deformation. *Bull. Earthquake Eng.* 8: 283-307.
- Bardet, J. P., Ichii, K. & Lin, C. H. (2000). EERA: A computer program for equivalent linear earthquake site response analysis of layered soils deposits. Los Angeles: University of Southern California.
- Benz, T. (2006). Small-strain stiffness of soils and its numerical consequences. PhD thesis, University of Stuttgart, Germany.
- Bransby, M. F., Brown, M. J., Knappett, J. A., Hudacsek, P., Morgan, N., Cathie, D., Maconochie, A., Yun, G., Ripley, A. G., Brown, N. & Egborge, R. (2011). Vertical capacity of grillage foundations in sand. *Can. Geotech. J.* 48(8), 1246–1265, DOI: 10.1139/t11-040.
- Chopra, AK. (2001). Dynamics of structures: Theory and applications to earthquake engineering. Englewood Cliffs, NJ: Prentice Hall.
- Dowding CH, Rozen A (1978). Damage to rock tunnels from earthquake shaking. *J Geotech Eng Div* 104(GT2):175–191.
- Hardin, BO. & Drnevich, VP (1972). Shear modulus and damping in soils: design equations and curves. *J. Soil Mech. Found. Div.*, ASCE 98(SM7): 667–692.
- Hashash YMA, Hook JJ, Schmidt B, Yao JI-C (2001) Seismic design and analysis of underground structures. *Tunnel Undergr Space Technol* 16(2):247–293.
- Iida H, Hiroto T, Yoshida N, Iwafuji M (1996) Damage to Daikai subway station. Special issue on geotechnical aspects of the January 17 1995 Hyogoken–Nambu earthquake. *Soils Found* 283–300.
- Kawashima, K (1999). Seismic design of underground structures in soft ground, a review. *Proceedings of the International Symposium on Tunnelling in Difficult Ground Conditions*. Tokyo, Japan.
- Knappett, JA, Madden, P, and Caucis, K (2015). Seismic structure-soil-structure interaction between pairs of adjacent building structures. *Geotechnique* 65(5): 429-441.
- Kontoe, S, and Zdravkovic, L, Potts DM, and Menkiti, CO (2011). On the relative merits of simple and advanced constitutive models in dynamic analysis of tunnels. *Geotechnique*, 61(10): 815-829.
- Kwok AOL, Stewart JP, Hashash YMA, Matasovic N, Pyke R, Wang Z (2007). Use of exact solutions of wave propagation problems to guide implementation of nonlinear seismic ground response analysis procedures. *J Geotech Geoenviron Eng* 133(11): 1385–98.
- Lanzano, G Bilotta, E, Russo, G, and Silvestri, F (2015). Experimental and numerical study on circular tunnels under seismic loading. *European Journal of Environmental and Civil Engineering*, 19(5):539-563.
- Lauder, K, Brown, MJ, Bransby MF & Boyes S (2013) The influence of incorporating a forecutter on the performance of offshore pipeline ploughs. *Applied Ocean Research Journal*, 39: 121–130.
- Lysmer, J. & Kuhlmeyer, RL (1969). Finite dynamic model for infinite media. *ASCE J. Engng Mech. Div.* 95(4): 859–887.
- Nakamura S, Yoshida N, Iwatate T (1996) Damage to Daikai subway station during the 1995 Hyogoken–Nambu earthquake and its investigation. *Japan Society of Civil Engineers, Committee of Earthquake Engineering*: 287–295.
- Newmark, NM (1959). A Method of Computation for Structural Dynamics. *ASCE Journal of Engineering Mechanics Division*, 85(EM3).
- O’ Rourke TD, Goh SH, Menkiti CO, Mair RJ (2001). Highway tunnel performance during the 1999 Düzce earthquake. In: *Proceedings of the 15th International Conference on Soil Mechanics and Geotechnical Engineering*, August 27–31, Istanbul.
- PLAXIS 2D. Manual; 2016.
- Santos, JA & Correia, AG (2001). Reference threshold shear strain of soil: its application to obtain a unique strain-dependent shear modulus curve for soil. *Proceedings of the 15th international conference on soil mechanics and geotechnical engineering*, Istanbul, Turkey, 1: 267–270.
- Schanz, T, Vermeer, PA & Bonnier, PG (1999). The hardening soil model: formulation and verification. In *Beyond 2000 in computation geotechnics* (ed. R. B. J. Brinkgreve), pp. 281–290. Rotterdam, the Netherlands: Balkema.

- Smith, IM., Griffiths, DV (1982). *Programming the Finite Element Method*. John Wiley & Sons, Chisester, U.K., second edition.
- Tsinidis G, Ptilakis K, Anagnostopoulos C (2016a). Circular tunnels in sand: dynamic response and efficiency of seismic analysis methods at extreme lining flexibilities. *Bull Earthq Eng* 14: 2903–29.
- Tsinidis, G., Ptilakis, K., Madabhushi, G (2016b). On the dynamic response of square tunnels in sand. *Engineering Structures* 125: 419–437.
- Ueng, TS, Lin ML, Chen MH (2001). Some geotechnical aspects of 1999 Chi-Chi, Taiwan earthquake. *Proceedings of the Fourth International Conference on Recent Advances in Geotechnical Earthquake Engineering and Soil Dynamics*. SPL-10.1(5): 1-5
- Wang, JN (1993). *Seismic design of tunnels: A state-of-the-art approach*, Monograph 7. New York: Parsons, Brinckerhoff, Quade and Douglas, Inc.
- Zerwer, A, Cascante, G & Hutchinson, J (2002). Parameter estimation in finite element simulations of Rayleigh waves. *J. Geotech. Geoenviron. Engng* 128(3): 250–261.